University Research to Support the MPACT 2020 Milestone

Noah C. Harris[1], Haori Yang[1], Jianbang Ge[2], Jinsuo Zhang[2], Jamie Coble[3], Steve Skutnik[3], Neil R. Taylor[4], Joshua Jarrell[4], Thomas E. Blue[4], Lei Cao[4], Michael Simpson[5], Benjamin B. Cipiti[6], Nathan Shoman[6]

[1]Oregon State University
Corvallis, OR USA

[2]Virginia Polytechnic Institute
Blacksburg, VA USA

[3]University of Tennessee
Knoxville, TN USA

[4]Ohio State University
Columbus, OH USA

[5]University of Utah
Salt Lake City, UT USA

[6]Sandia National Laboratories
Albuquerque, NM USA

Abstract
University research is a strong focus of the Office of Nuclear Energy within the U.S. Department of Energy. This research complements existing work in the various program areas and provides support and training for students entering the field. Four university projects have provided support to the Material Protection Accounting and Controls Technologies (MPACT) 2020 milestone focused on safeguards for electrochemical processing facilities. The University of Tennessee Knoxville has examined data fusion of Non-Destructive Analysis (NDA) measurements such as Hybrid K-Edge Densitometry and Cyclic Voltammetry. Oregon State University and Virginia Polytechnic Institute have examined the integration of accountancy data with process monitoring data for safeguards. The Ohio State University and the University of Utah have developed a Ni-Pt SiC Schottky diode capable of high temperature alpha spectroscopy for actinide detection of molten salts. This paper presents an overview of this work and how these technologies or approaches may tie into an overall safeguards approach.

Introduction
University research to support the MPACT program has focused on supporting the Virtual Facility Distributed Test Bed which is described in an accompanying paper in this issue. The Virtual Facility Distributed Test Bed was developed as part of a 2020 milestone to demonstrate complete Safeguards and Security by Design (SSBD) for future nuclear fuel cycle facilities using the integrated capabilities of MPACT. The university research described here contributes to the "high fidelity capabilities" and includes new safeguards data analytics approaches and new

measurement technologies which contribute to the proposed safeguards approach for electrochemical facilities.

The University of Tennessee Knoxville has analyzed the integration of data sources for improved safeguards and process monitoring. New measurement models were developed for integration with the safeguards modeling capability used in the MPACT program. This work explores alternative materials accountancy approaches in case the measurement technologies are not able to meet safeguards goals.

A joint project between Oregon State University and Virginia Polytechnic Institute, still ongoing, is examining the integration of process monitoring information with materials accountancy to explore new safeguards approaches for electrochemical facilities. This work is evaluating radiation signatures from Non-Destructive Analysis (NDA) measurements to reduce reliance on Destructive Analysis (DA). In addition, an electrochemical method is being developed for determining ion concentrations in a molten salt system. This project also examines alternative safeguards approaches that may reduce reliance on DA.

A joint project between The Ohio State University and the University of Utah has developed a 320 μm thick 4H-SiC Schottky diode, using a 100-nm nickel contact and 10-nm platinum as a corrosion barrier layer that are fully packaged into a rugged device, as an alpha radiation sensor for a high temperature and corrosive molten salt environment. The goal of this work is to develop a detection system for measuring actinide concentrations in a molten salt. The measurement of actinides in the electrorefiner is a key goal for materials accountancy.

Finally, the University of Colorado has worked with Los Alamos National Laboratory to develop a key enabling technology for the Microcalorimeter, which is being examined as a new NDA measurement technology. This work is not described here but is described in more detail in an accompanying paper in this journal issue.[1]

Integration of Data Sources for Improved Safeguards and Process Monitoring

Material Control & Accountability (MC&A) programs at nuclear processing plants deter and detect theft and diversion of nuclear material by both outside and inside adversaries. Current destructive assay approaches to MC&A can be augmented with nondestructive assay and online process monitoring measurements to reduce the required resources and improve the timeliness of alerts and decision making. Model-based methods to correlate process measurements with declared operations have been suggested for additional robustness in facility assessment and proliferation detection.[2] Multiple process monitoring measurements may be available for monitoring electrochemical reprocessing systems, including salt density, level, actinide concentrations, cathode voltage, and temperature. These process monitoring signals can be combined with traditional material accountancy measurements (such as passive NDA techniques) to provide more accurate and timely accountancy during process operation.

Statistical data analysis and modeling extract actionable knowledge from streams of seemingly disparate data. Data fusion algorithms common in other domains can be applied to the

electrochemical safeguards and monitoring measurements to provide reliable, robust, and timely indicators of potential anomalies or misuse. Because fuel reprocessing is a well-controlled, repeatable series of process steps, the expected behavior across the system could be established for a variety of fuel types and characteristics. Multivariate analysis methods common in chemometrics act as pattern recognition techniques, which can detect small deviations from the expected, nominal process conditions. Previous work has applied modeling techniques such as principal component analysis and partial least squares regression to gamma spectra for monitoring and detection in aqueous reprocessing systems.[3] Other empirical modeling methods are commonly applied for process monitoring and anomaly detection in industrial systems and chemical processes.[4]

Previously developed electrochemical processing flowsheet models, such as the Separations and Safeguards Performance Model-Electrochemical (SSPM EChem), track elemental and bulk material flows through various unit operations,[5] providing a basis from which to evaluate the safeguards requirements of and design new accountancy systems for electrochemical reprocessing plants. Work at the University of Tennessee focused on augmenting these flowsheet models with simulations of relevant measurement methods to generate data necessary to develop and demonstrate process monitoring for safeguards. The augmented electrochemical processing flowsheet model can be used to simulate measurement data under a variety of normal and diversion conditions. Similarly, the incorporation of physical measurement models with high-fidelity source terms into the safeguards model facilitates the ability to evaluate marginal contributions for the placement and sampling frequency of different measurement systems to meet facility measurement goals (including standard error of inventory difference). Such a capability aids in understanding the impact of new measurement techniques developed in the future as they are incorporated into the safeguards model.

Candidate Measurement Techniques

A survey of the relevant measurements that are available, under development, or proposed for electrochemical reprocessing systems identified twenty-two measurement modalities relevant to online monitoring in electrochemical reprocessing facilities.[6] Proposed measurement methods available in the open literature were reviewed and evaluated according to the potential information or indicator(s) gleaned from each measurement, the latency period (that is, a qualitative indication of the time needed to complete a single measurement), potential locations for measurement deployment, and the estimated uncertainty associated with the measurement. The surveyed measurement techniques were classified into three categories: passive radiation signatures, active radiation signatures, and control and process state variables.

In addition, the measurements were evaluated in the context of the SSPM EChem model to determine if the information needed to simulate measurement response would be available. Of the twenty-two measurement methods considered, twelve are potentially amenable to integration in the SSPM EChem model using information that is already available or easily added to that flowsheet model. Of those, four were chosen for demonstration of this simulation and integration including: gamma emissions, neutron emissions, hybrid k-edge densitometry, and cyclic voltammetry.

Measurement Integration in SSPM

Data analytics routines and empirical modeling are attractive for process monitoring and accountancy because they do not require high-fidelity models of the physics of the system and measurement modalities. However, development and evaluation of these methods require the availability of potentially significant quantities of representative data. In the case of electrochemical used nuclear fuel reprocessing, system measurements under normal and off-normal conditions covering the range of potential fuel compositions and postulated upset conditions are not available for commercial-size facilities. To develop and demonstrate process monitoring for electrochemical reprocessing facilities, representative data must be simulated based on the physics of both the indicator being measured and the measurement technique. In order to provide data to support development of data analytics-based approaches to safeguards and process monitoring, simulation models of key *in situ* process monitoring measurements were developed and implemented in the MATLAB-Simulink environment to integrate with a previously-developed electrochemical processing simulation model, the SSPM EChem.

SSPM EChem tracks elemental, isotopic, and bulk material flow through the electrochemical processing flowsheet. With these physical features available to describe the operation of the facility, a variety of radiation- and non-radiation-based signatures were simulated. Figure 1 summarizes the simulation approach taken in this research, from source term development through *in situ* simulation of key process monitoring signatures.[7] Many radiation-based signatures, such as gamma and neutron emissions and hybrid k-edge densitometry (HKED), can be estimated from the elemental and isotopic concentrations already tracked in SSPM EChem. Additional signatures, such as cyclic voltammetry (CV) or spectroscopy, require knowledge of the concentration oxidation states of key elements. Four signatures are simulated in SSPM-EChem: passive gamma emissions, passive neutron emissions, HKED, and CV. These signatures were selected for this proof of concept implementation due to their compatibility with the information tracked in SSPM-EChem, namely elemental and isotopic masses. For brevity, the mathematical formulations of these signatures are not repeated here. Detailed presentations of the simulation approaches can be found in reference 8 (gamma and neutron emissions) and reference 9 (HKED).

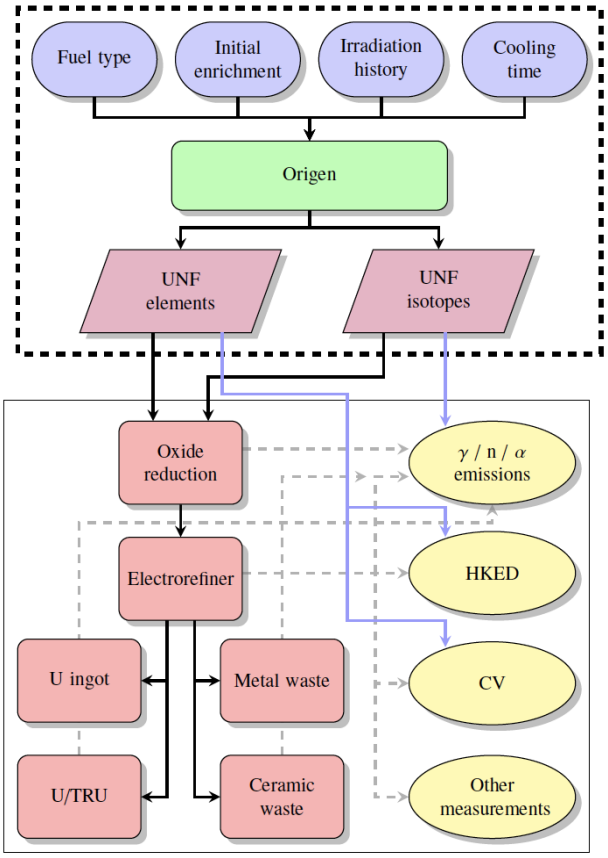

Figure 1. Overview of physical signature simulation in the Echem SSPM.[7]

Measurement Analytics for Safeguards

In addition to simulating the expected measurement response, measurement uncertainty and error propagation estimates were evaluated for both HKED and CV. The excellent performance of HKED measurements for aqueous reprocessing has led to interest in the application of HKED for pyroprocessing applications. Experimental studies are limited and there are several challenges for creating computational models.

The analysis of simulated online process monitoring data follows three tracks: confirmatory measurements, material characterization, and process monitoring for diversion detection. Confirmatory measurements primarily consist of passive radiation detectors at locations that should not have significant radiation emissions. If a signal is measured above the expected background, a simple threshold will alert the operators or inspectors to unexpected facility operation. This is a simple application of existing technology and techniques and is not explored here in detail. The use of online monitoring signals for direct, non-destructive characterization of material composition and for unsupervised anomaly detection are of greater interest in the current research.

Several measurement modalities can directly provide information about the composition of materials at key stages in the electrochemical reprocessing facility. This research focused on

characterizing material composition at the electrorefiner, though some of the proposed methods may be applicable in other stages.

By combining the uranium mass fraction indicated by k-edge densitometry (KED) with the plutonium-to-uranium ratio found through x-ray fluorescence (XRF), HKED can give a direct estimation of the plutonium mass fraction in the electrorefiner salt. Exemplary results of this estimation for one fuel type over a 600-hour run are shown in Figure 2. To add realism to this simulated result, Gaussian noise is added to both the k-edge drop used to estimate the uranium mass fraction and to the XRF peaks used to estimate the plutonium-to-uranium mass fraction. Note that the true P/U fraction modeled in the SSPM follows a step transition as new batches of fuel are processed. Around hour 300, extraction of the U/TRU product begins and a somewhat steady-state condition is reached. The values increase and decrease due to the timing of batches.

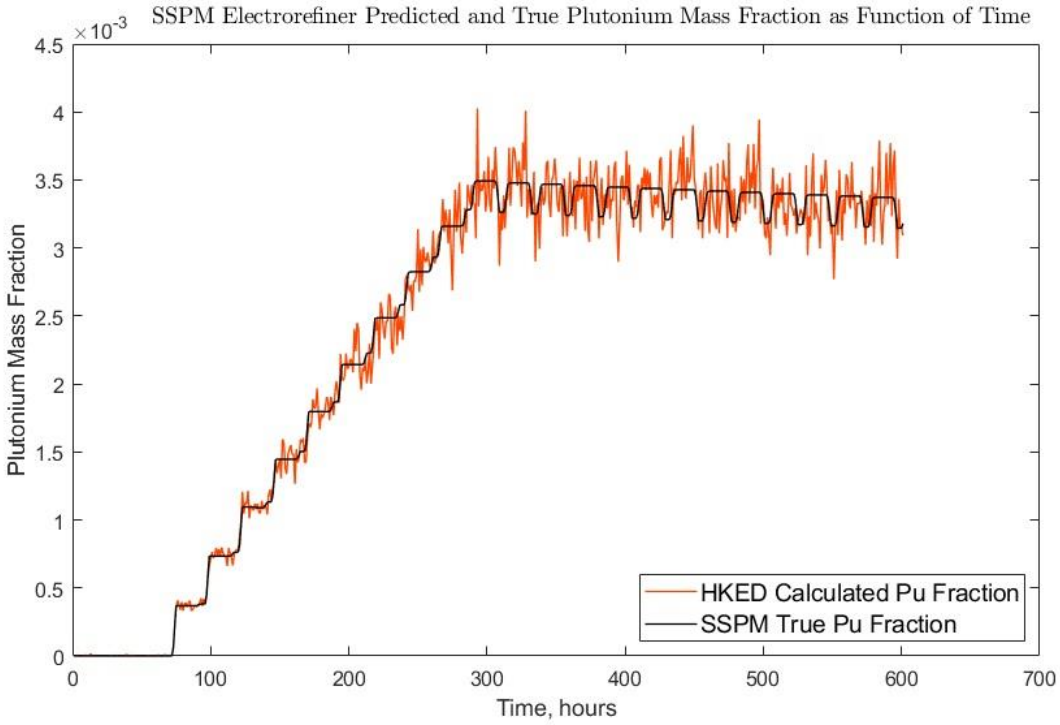

Figure 2. Exemplar of HKED estimated Pu mass fraction in the electrorefiner over a 600 hour run. Fuel is 2.6% enriched and discharged at 33 GWd/MTU.[9]

The SSPM HKED measurement model was based on an empirical fit of results from high fidelity MCNP calculations. However, the overall measurement uncertainty, largely driven by counting statistics in the MCNP calculation, was 4.86%. This is approximately an order of magnitude larger than the uncertainty seen in experimental measurements, which can be as low as 0.5% for aqueous solutions. The measurement uncertainty of the empirical fit is close to the uncertainty of NDA measurements of plutonium, which is about 5%. These measurement uncertainties are too high for many safeguards applications outside of confirmatory measurements; managing these numeric uncertainties is an area of ongoing need to provide reasonable and realistic simulated data to support development of process monitoring-based safeguards approaches.

CV results can also be related to the uranium weight percent in the electrorefiner through correlation models, as suggested in reference 10. For implementation in SSPM-EChem, CV peaks in the irreversible region were numerically simulated using equations and data from reference 11. A piecewise linear function was fitted to simulated peak differences to relate the peak difference to U weight percent.[12] Figure 3 shows the result of this estimation over time in the SSPM EChem simulation. The actual modeled values start with an initial salt loading and then decrease slightly as the fuel is processed. The current balance of uranium on the cathode must equal the total current of fuel going into the salt (uranium plus transuranics and fission products), so the uranium concentration values drop slightly with each batch. Periodically, UCl_3 is added back in to bring the concentrations back up. The model does not quite reach steady-state by 1000 hours. Here, the CV-based estimation consistently underestimates the uranium weight percent, although this could potentially be improved with a more accurate model to relate key features of the CV trace to the uranium weight percent.

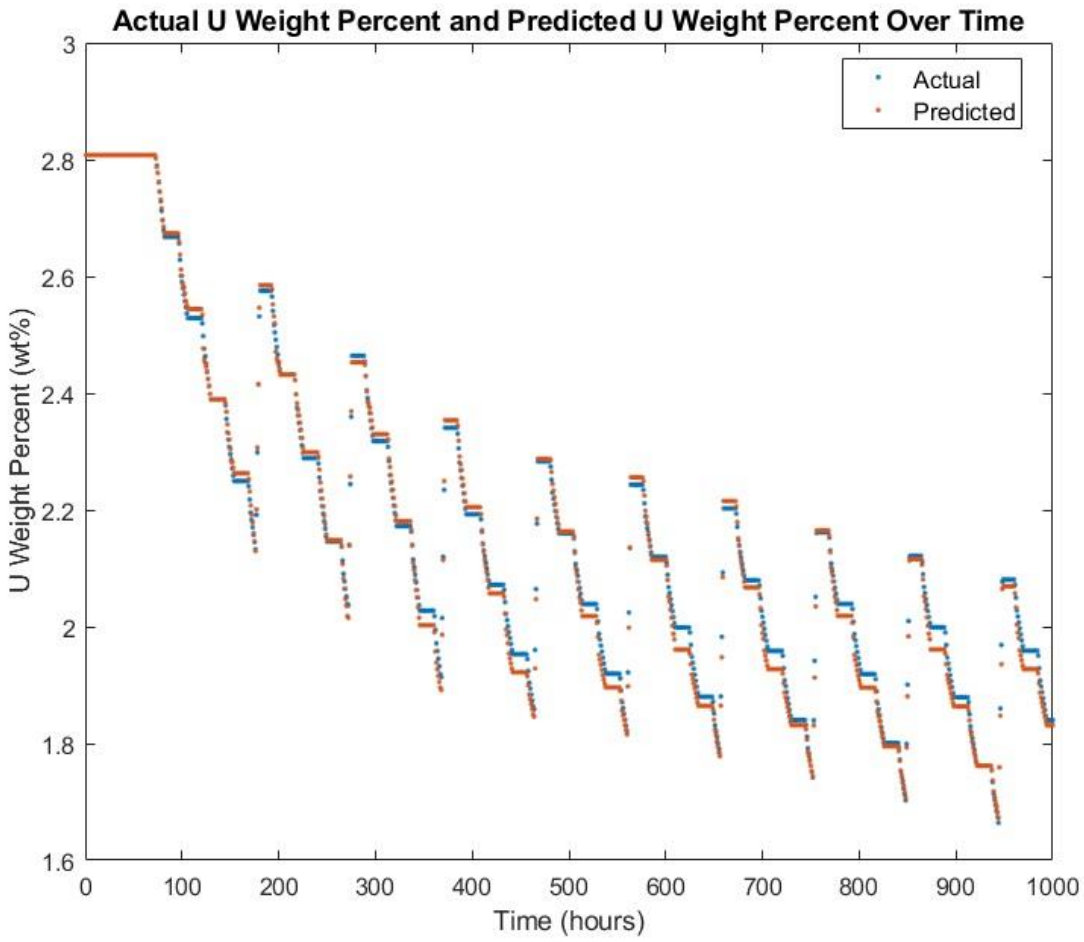

Figure 3. Uranium weight percent in the electrorefiner indicated by cyclic voltammetry during a 1000 hour run.

Four measurement modalities have been implemented in SSPM-EChem to demonstrate the capability to generate relevant in situ measurements for safeguards applications. Simulated signatures are contaminated with noise from both numeric simulation and realistic measurement

specifications in the open literature. Future work could extend this approach to include additional measurements to support development of an autonomous process monitoring and data-driven safeguards approach.

Integration of Radiation Signatures and Electrochemical Monitoring

The work of Oregon State University[13] is examining the use of NDA measurements for electrochemical safeguards. This work uses the Gamma Detector Response and Analysis Software (GADRAS)[14] and the SSPM[5] to predict the difference in radiation signatures between normal and diversion scenarios for various source term geometries. In parallel, the work with Virginia Polytechnic Institute is developing an electrochemical method to determine actinide concentrations in molten salts.

NDA for E-Chem Safeguards

There are many measurement points available in the SSPM schema, and it is important to understand how NDA techniques fit into the larger picture. Microcalorimetry and the High Dose Neutron Detector (HDND) are novel NDA technologies being developed by the MPACT campaign for accountancy at various locations in an electrochemical processing facility. These NDA measurements will most likely be applied to the metal waste form, fission product waste, and input accountancy. These technologies could also likely be extended to the uranium and transuranic product ingots through further investigation.

The Gamma Detector Response and Analysis Software (GADRAS) is a software suite developed at Sandia National Laboratories, which is capable of performing source term modeling and one-dimensional radiation transport for generation of gamma and neutron signatures. The GADRAS C# API was used to build software capable of taking output data from the SSPM, in the form of full isotopic vectors (1675 isotopes), down selecting only the isotopes which are of interest as gamma or neutron sources, turning them into GADRAS models with various geometries, running transport and detector response calculations on those models, and then finally analyzing the resulting spectra and count rates.

Figure 4 is a sample dataset produced by the software, comparing a normal (control) scenario with a material loss scenario. The fuel source term was simulated with a 33 GWd/MTHM burnup at 2.60% enrichment. The loss scenario was a direct, abrupt removal of electrorefiner salt around hour 1600 in the SSPM, which corresponds to approximately 8 kg of diverted Pu (one significant quantity, or SQ). An abrupt loss means that the material is removed all within one material balance period. Spherical geometry was used at all the key measurement points (KMPs) with 10cm, 150cm, 25cm, and 10cm lead shielding used for the U product, U/TRU product, fission product waste, and metal waste measurements respectively. There are four series that represent the simulated measurement from the control and loss cases for the four measurement points. All measurement points show discrepancies in the total gamma count rates due to the material loss and show the potential value of utilizing this approach for detection.

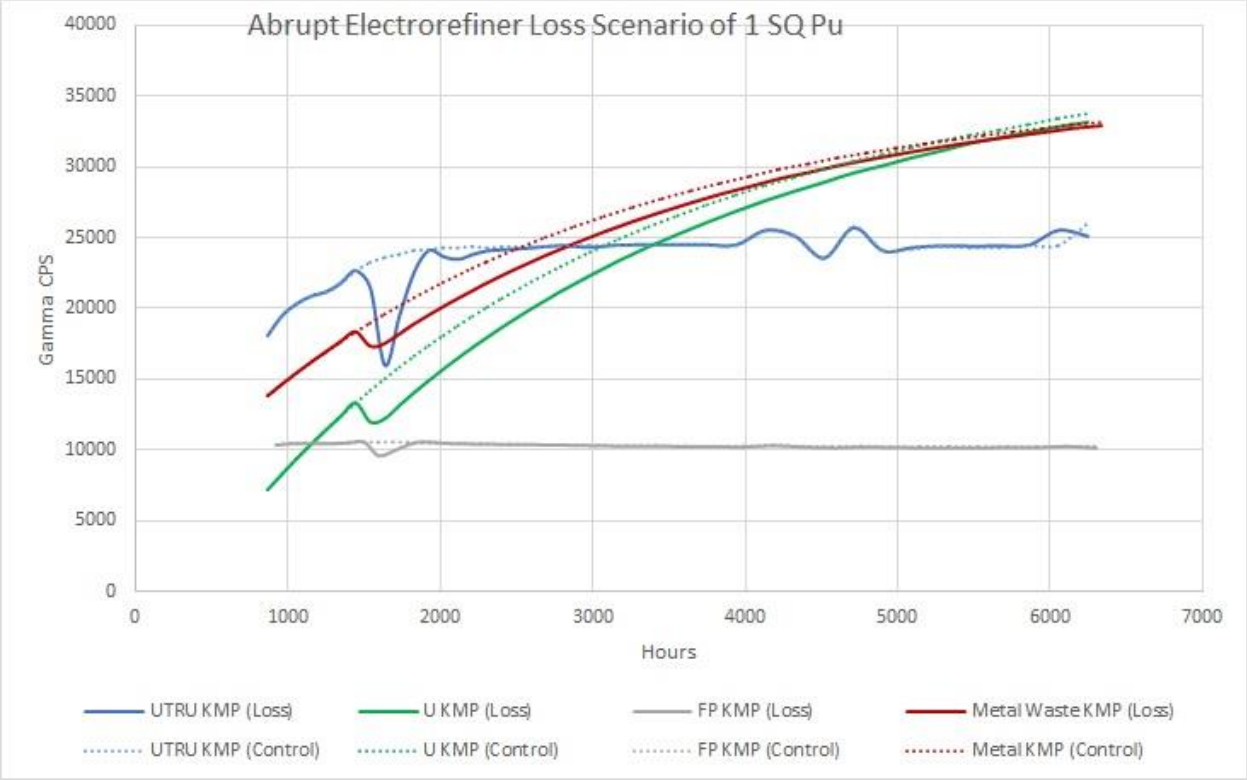

Figure 4. Normal and diversion datasets for an abrupt ER diversion starting at hour 1600.

Two protracted loss scenarios were also examined to demonstrate the lower limits of what may be detectable via NDA. In both cases, 1 SQ of Pu was removed from the electrorefiner and transuranic product processing over a longer period of time (greater than one material balance period). The results are shown in Figures 5 and 6 respectively.

For the protracted electrorefiner loss (Figure 5), there are a few noteworthy points. The first is that the metal waste form and uranium product processing KMPs appear to be the most useful for detecting a protracted loss, as their values steadily diverge from the control scenario over the course of the loss. By the end of the loss period the metal waste showed a discrepancy of 2100 counts per second (CPS) and the uranium processing a discrepancy of 2800 CPS. The latter is over 10 standard deviations with the detectors operating at around 33,000 CPS. The standard deviation (for testing the null hypothesis) is $\sigma = \sqrt{2}\sqrt{33000} = 257$.[15] Assuming proportionality between loss amount and count discrepancy, there is a 99% confidence in detecting a 0.2 SQ loss via $\frac{2.58\,\sigma}{2800} = 0.24$.

The fission product (FP) KMP did not prove to be very useful for detecting this ER loss, and the transuranic (U/TRU) KMP displayed an oscillatory behavior, which is most likely due to changes in rare earth fission products from drawdown operations. Both of these measurements do not appear to be useful for detection.

For the transuranic product loss (Figure 6), the only relevant KMP was the transuranic NDA measurement. This makes sense as there are very few KMPs after the loss location, unlike for the

electrorefiner loss. For the duration of this loss, there is a consistent discrepancy between the control and loss scenarios with an average CPS difference of approximately 400. The detectors are running a total CPS of around 24,000. Thus, the standard deviation (for testing the null hypothesis) is $\sigma = \sqrt{2}\sqrt{24000} = 219$. For just one measurement point a confidence interval of around 93% is obtained.[14] Over the course of this loss, there may be as many as 60 measurement points. Research into the statistical implications of having so many measurement points is ongoing. To obtain a confidence interval of 99% one could multiply the standard deviation by 2.58.[15] 2.58*219 = 565. This discrepancy would correspond to a loss of 1.4 SQ if proportionality between loss amount and count rate is assumed.

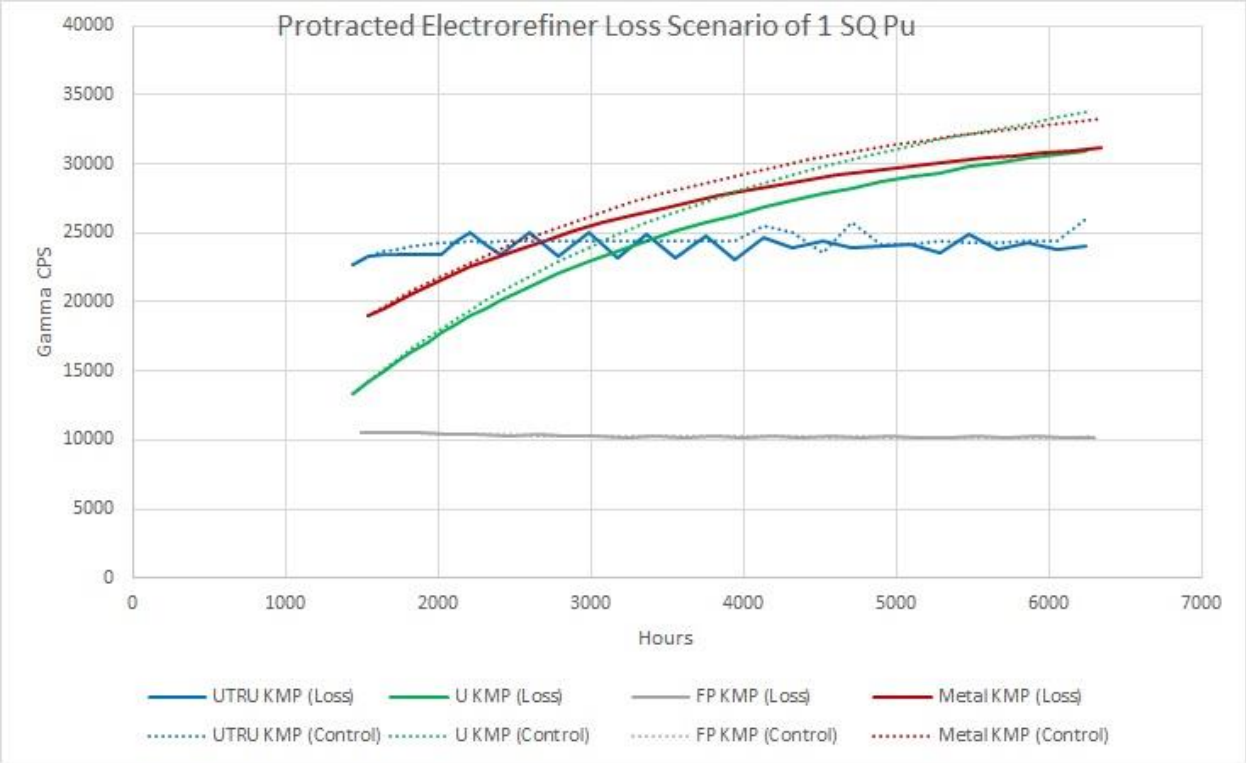

Figure 5. A protracted loss scenario from the electrorefiner

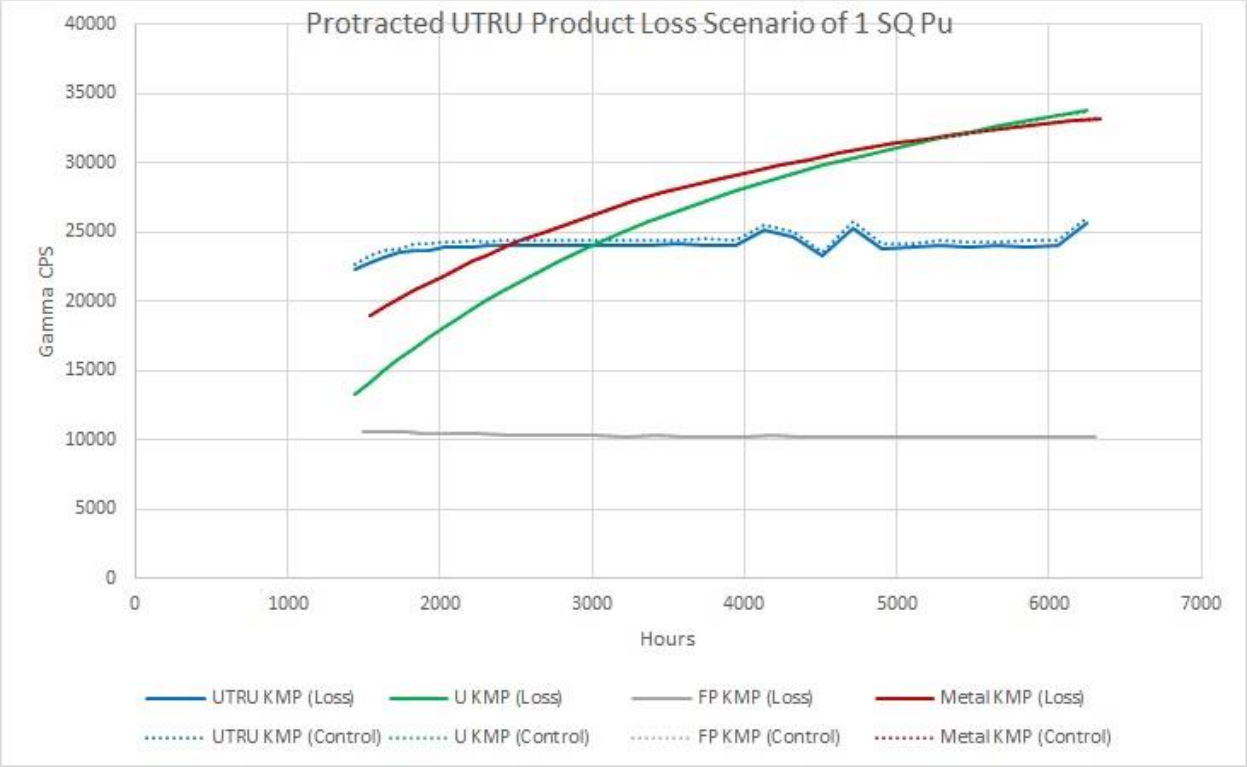

Figure 6. A protracted loss scenario from the U/TRU product

Current efforts have been focused on development of various software tools. Future work will focus on analysis of additional SSPM simulations to clarify the detection discrepancies for various loss scenarios (abrupt and protracted) that correspond to roughly one significant quantity of plutonium being diverted. In addition, the modeling work shown here assumed constant source terms for the spent fuel—future work will need to examine how changing source terms may affect the ability to detect material loss. Preliminary results have shown positively that total gamma count can be used to measure certain diversion scenarios, so what remains is to get a handle on the huge amount of potential data available for study.

Integrating this work into the SSPM will require some additional software beyond MATLAB. GADRAS, Microsoft Visual Studio, and Microsoft Excel would need to be better integrated. The flexibility and automation of analysis should justify the larger software overhead.

Other electrochemical measurements should prove easier to integrate into the virtual test bed. An example of work which will fit more cleanly into the test bed as a MATLAB Simulink block is being carried out by Virginia Tech, an electrode sensor model for the electrorefiner unit.

Experimental Work: Electrochemical Measurements

The electrochemical sensor measures ion concentration in a static molten salt based on a CV scan. However, there is molten salt flow that mixes the salt in most electrorefiners,[10] and the CV signals in a static molten salt are different from these in a flowing molten salt. Therefore, it is

necessary to develop an innovative method to enable an electrochemical sensor to measure ions such as U^{3+} concentration in a flowing molten salt.

In the present work, a graphite rotating disc electrode (RDE) was designed to simulate the molten salt flow,[16] and then the concentrations and diffusion coefficients of Eu^{3+} and Eu^{2+} in molten LiCl-KCl were determined. Eu was selected as an example element because it is known that Eu^{3+} and Eu^{2+} are stable ions in molten KCl-LiCl. With the graphite RDE, the limiting currents of the reduction of Eu^{3+} and the oxidation of Eu^{2+} were measured at various rotating speeds. The concentration ratio of Eu^{3+}/Eu^{2+} was changed through chronoamperometry electrolysis. Then the concentrations and diffusion coefficients of Eu^{3+} and Eu^{2+} ions were calculated based on the Levich equation.[13]

A three-electrode system was applied in the electrochemical experiments for the study of LiCl-KCl-$EuCl_3$. The counter electrode and reference electrode were graphite rods. A graphite rod with a diameter of 6 mm was selected as the working electrode material. The boron nitride tube was selected as the insulation material due to its thermal stability and poor wetting properties by the salt. The graphite rod was inserted into the boron nitride tube with exacting tolerances. Prior to its use, this graphite RDE was screwed onto a SS303 shaft (Figure 7). When the salt system reached the equilibrium, the electrodes were carefully loaded into the melt. In this study, both cyclic voltammetry (CV) and chronoamperometry (CA) were performed to study the electrochemical behavior of Eu^{3+}/Eu^{2+}. The concentration ratio of Eu^{3+}/Eu^{2+} will be calculated using the Levich equation

$$i_L = 0.62\mathrm{nFA}D_o^{2/3}w^{1/2}v^{-1/6}C_o^* \quad (1)$$

Where i_L is the limiting current; n is the number of electrons involved in the electrode reaction; F is the Faraday constant; D_o is the diffusion coefficient of the analyte, O. A is the electrode area; w is the angular frequency of rotation; v is the kinematic viscosity of the LiCl-KCl salt, 0.0142 cm/s^2 at 773 K; C_o^* is the concentration of the analyte, O.

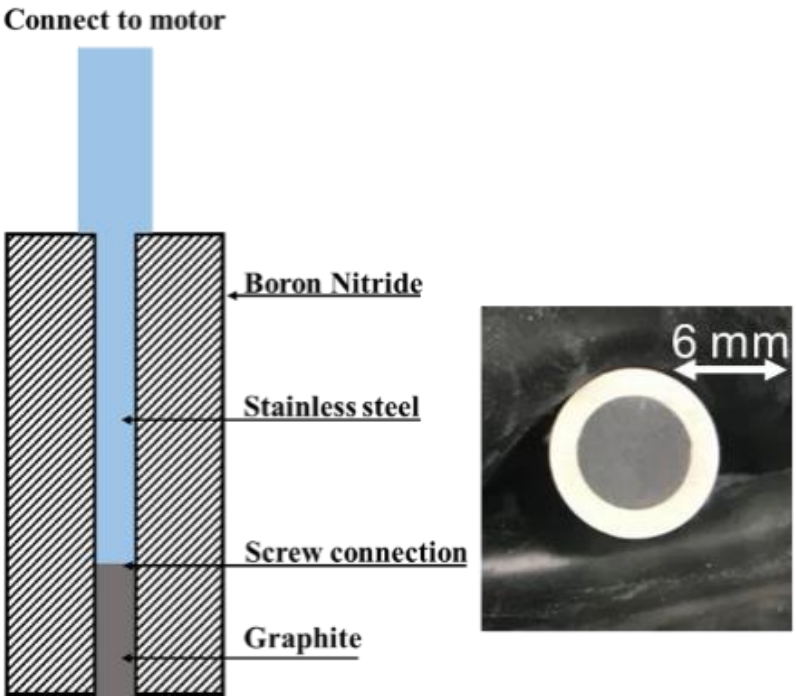

Figure 7. Schematic diagram and digital picture of graphite RDE

The graphite RDE was tested in the blank LiCl-KCl salt. The CV curves (Figure 8a) obtained without rotation showed very small residual currents. The range tested was chosen to examine the Eu^{2+}/Eu^{3+} ratio. Reduction of Li is more negative and was not run in this case. These peaks at 2100 and 2400 rpm should be related to the absorption of impurities in the blank LiCl-KCl salt. A series of CA tests (Figure 8b) at 1800 rpm were further conducted for 120 s to reveal the formation mechanism of these peaks. The current increased with the applied potential and these CA tests proved that the peaks in CV tests were not controlled by mass transfer. Moreover, the currents in CA tests (from -0.22 mA/cm^2 to 0.06 mA/cm^2) showed the high purity of the salt. With the addition of 0.5wt% $EuCl_3$, CV test was conducted to study the electrochemical behavior of the Eu^{3+}/Eu^{2+} redox couple. At 1800 rpm, the reduction current reached its limit (17.4 mA/cm^2) at -0.6 V *vs.* graphite (Figure 8c, dark line). The reduction current is related to the reduction of Eu^{3+} to Eu^{2+}. A platform of oxidation current was also observed even though the current started to increase at a more positive potential. The current platform was related to the limit of Eu^{2+} to Eu^{3+}. The oxidation and reduction currents proved the coexistence of Eu^{3+} and Eu^{2+} in the salt. A series of CA tests was also conducted to verify the accuracy of the limiting currents from CV tests, and the results are shown in Figure 8d. The CA test was first conducted at -0.6 V and the reduction current reached a steady value of 17.2 mA/cm^2, which was consistent with that from CV result. Thus, CV results can be used to determine the limiting currents. The steady currents obtained at -0.5 V and -0.6 V were 17.0 and 17.2 mA/cm^2 respectively, indicating the applied potentials were in the limiting current region. The CV test after CA tests in Figure 8c showed that CA tests could change the salt composition. Based on the Levich equation, the diffusion coefficients of $D_{Eu^{3+}}$ and $D_{Eu^{2+}}$ as well as their concentrations could be obtained by solving the equations:

$$i_{c1,l} = 0.62\mathrm{nFA}D_{Eu^{3+}}^{2/3} w^{1/2} v^{-1/6} C_{Eu_1^{3+}}^{*} \quad (2)$$

$$i_{o1,l} = 0.62\mathrm{nFA}D_{Eu^{2+}}^{2/3} w^{1/2} v^{-1/6} C_{Eu_1^{2+}}^{*} \quad (3)$$

$$i_{c2,l} = 0.62\mathrm{nFA}D_{Eu^{3+}}^{2/3} w^{1/2} v^{-1/6} C_{Eu_2^{3+}}^{*} \quad (4)$$

$$i_{O2,l} = 0.62\mathrm{nFA}D_{Eu^{2+}}^{2/3} w^{1/2} v^{-1/6} C_{Eu_2^{2+}}^{*} \quad (5)$$

$$C_{Eu_1^{3+}}^{*} + C_{Eu_1^{2+}}^{*} = C_{EuCl_3}^{*} \quad (6)$$

$$C_{Eu_2^{3+}}^{*} + C_{Eu_2^{2+}}^{*} = C_{EuCl_3}^{*} \quad (7)$$

Where $C_{Eu_1^{3+}}^{*}$ and $C_{Eu_2^{3+}}^{*}$ represent the concentration of $EuCl_3$ before and after CA tests, respectively; $C_{Eu_1^{2+}}^{*}$ and $C_{Eu_2^{2+}}^{*}$ represent the concentration of $EuCl_2$ before and after CA tests, respectively; $D_{Eu^{3+}}$ and $D_{Eu^{2+}}$ represent the diffusion coefficient of $EuCl_3$ and $EuCl_2$, respectively;$i_{c1,l}$, $i_{o1,l}$, $i_{c2,l}$ and $i_{O2,l}$ represent the measured limiting current. Thus, the calculated diffusion coefficients of $EuCl_3$ and $EuCl_2$ at 1800 rpm were $9.31*10^{-5}$ cm^2/s and $9.65*10^{-5}$ cm^2/s, respectively. The initial ratio of Eu^{3+}/Eu^{2+} was calculated to be 2.37. The ratio of Eu^{3+}/Eu^{2+} after CA tests was calculated to be 1.56.

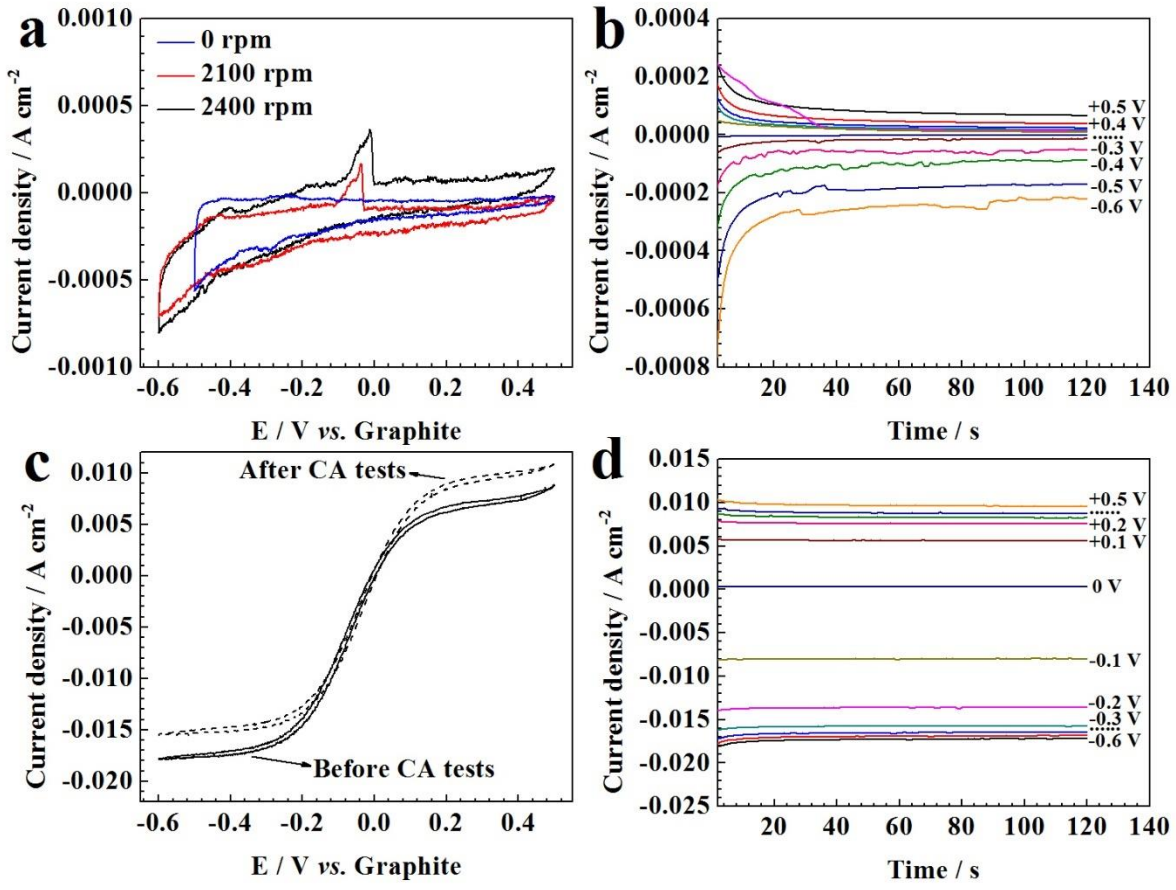

Figure 8. (a) CV tests in LiCl-KCl at various rotating speeds; (b) CA tests at various potentials for 120 s; (c) CV tests in LiCl-KCl-0.5wt% $EuCl_3$ before and after CA tests; (d) CA tests at various potentials for 120 s; Intervals: 0.1 V. Temp: 773 K. Scan rate and rpm: 20 mV/s and 1800. Total concentration of $EuCl_3$ (0.5 wt%) in LiCl-KCl salt: $3*10^{-5}$ mol/cm^3.

An RDE will be fabricated using inert metal electrode such as W, and then experiments will be performed for soluble-insoluble redox couples such as La^{3+}/La and U^{3+}/U to measure the ion concentration in molten KCl-LiCl. Based on experimental results, a relationship between the ion concentration and the molten salt flow velocity will be developed, which will be applied to obtain the ion concentration in a flowing molten salt based on signals measured by a 3-electrode electrochemical sensor.

Development of a Ni-Pt SiC Schottky Diode for Alpha Spectroscopy

Work at The Ohio State University and the University of Utah is focused on developing a method for near real-time monitoring of the concentrations of actinides in molten salt for an electrorefiner vessel. A detection system can be implemented that uses the measured spectrum of count rate vs. energy and the characteristic alpha emission energies from isotopes of special nuclear materials to determine the isotopic concentrations of the materials. The monitoring method is a two-step process. The purpose of the first step (the pre-concentration step) is to deposit actinides onto a diode detector's Schottky contact (strictly speaking on the tens of nm scale platinum corrosion barrier layer that covers the thin-film nickel contact); and the second step is to acquire an alpha particle energy spectrum after a thin-film of actinides has been plated on the detector's Schottky contact.[17] Then, the measured alpha emission rates can be divided by the published specific activities, for each actinide alpha decay peak, within the energy spectrum. This division yields the number of atoms of the isotope, which have been deposited on the detector's platinum surface, for the corresponding energy peak. With a knowledge of the collection volume and the collection efficiency, the concentration can be determined for each isotope of an actinide in the salt.

Such a two-step method has two principle advantages: 1) the pre-concentration step can be made to deposit the actinides selectively, by appropriately adjusting the electrode potential; and 2) as shown in Figure 9, if the detector has sufficiently good energy resolution, in the second step in the process, the deposited thin-film of alpha emitters can produce well-resolved peaks in the measured pulse height energy spectrum, without interference in the spectrum that would arise from events that are due to decays within the salt. Alpha particles that are born within the salt (as opposed to alpha particles that are born on the detector's platinum surface) are degraded in energy, as they traverse the distance from their origin in the salt to the platinum surface; thereby obscuring the peaks in the spectrum, that arise from the decay of isotopes that are deposited on the platinum, and thus significantly increasing the analytical uncertainties in the estimates of the isotopic concentrations of the materials that are dissolved within the salt.

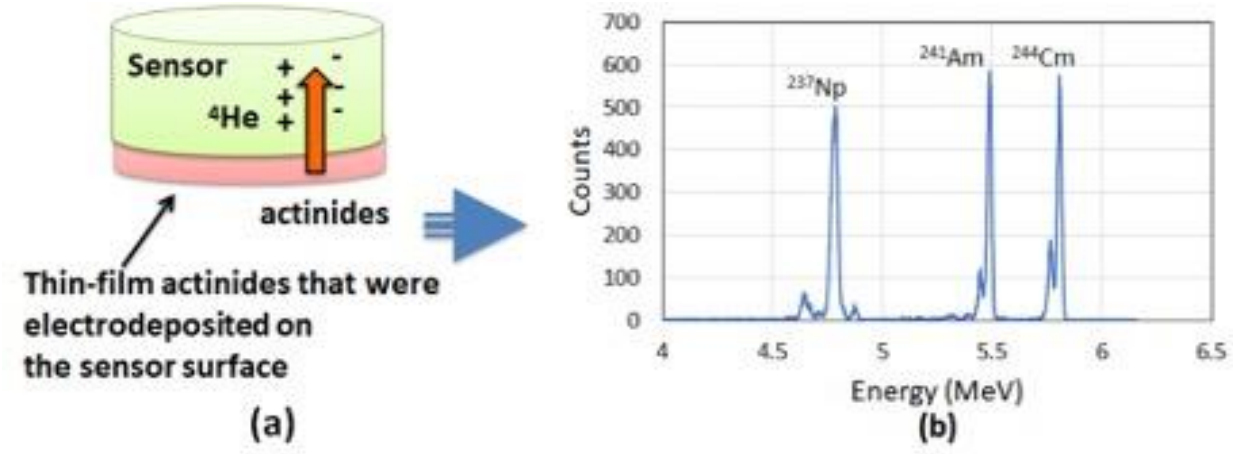

Figure 9. Actinides measurement based on alpha energy spectra with (a) pre-concentration step, (b) the subsequent well-resolved alpha energy peaks.

Another advantage of the two-step process is that in the pre-concentration step, as the radiation detector is submerged in a molten salt and a voltage is applied to selectively deposit an actinide of interest on its platinum surface, the elemental (not isotopic) concentration in the salt can be determined using chronoamperometry (which is an electrochemical characterization method).[18]

To operate a detector in the pyroprocessing environment, multiple design parameters must be considered. An electrorefiner has limited instrumentation ports on its top, thus supporting few compact detectors.[19] Thin-film solid state detectors have a low detection efficiency to gamma rays[20] from fission products in the salt. Additionally, the molten salt can be very reactive with certain materials. Therefore, a packaged detector must be devised that can withstand the molten salt environment and which is stable to at least 500 °C. While silicon-based detectors offer excellent energy resolution at room temperature, their leakage current is large at modest temperatures, due to thermal excitation. The corresponding increase in intrinsic carrier concentration at elevated temperatures and poor radiation hardness precludes their use for this application.

A polytype of silicon carbide possesses the necessary characteristics. 4H-SiC, a hexagonal crystalline form of SiC, has in recent years been grown in high purity and in the thickness necessary for alpha spectroscopy applications, on the order of micrometers.[21-24] 4H-SiC offers good stability at elevated temperature, good chemical stability in chloride salts, and is insensitive to gamma radiation, with good resolution for alpha spectroscopy.[21] Adding a Schottky contact on the SiC epilayer and an Ohmic contact on the SiC substrate allows for high temperature operation and rectifying behavior.[25] To resolve the alpha peaks of several common actinides that are found in spent nuclear fuel, it is necessary for a detector to have an energy resolution (the ratio of Full Width at Half Maximum (FWHM) to peak energy) of approximately 1-2%. Alpha detectors using 4H-SiC have been demonstrated, at approximately room temperature, to have energy resolution of less than 0.3% at 5.486 MeV.[26] Detectors using Schottky contacts and 4H-SiC, which have been designed to operate at or above 500°C, have been demonstrated to have energy resolution of approximately 18%.[27]

Device Fabrication

A 4H-SiC wafer was diced into 0.5 x 0.5 cm square dies. The wafer had a 21 µm thick epitaxial 4H-SiC layer, with a doping concentration of $5x10^{14}$ atoms/cm^3 of nitrogen that was deposited on a 300 µm thick 4H-SiC substrate, which was doped with $1x10^{18}$ atoms/cm^3 of nitrogen. The dies were cleaned on both their epitaxial and bulk surfaces, using an RCA (Radio Corporation of America) cleaning process to remove organic, ionic, and oxide contaminants.[28] A 100 nm thick nickel contact was deposited on the cleaned substrate surface, using an electron beam evaporator. A 10-nm platinum layer was deposited on the nickel surface to serve as a protective layer against oxidation of the nickel layer and to provide a good electrical contact.

Next, the die was annealed at 950°C to form an ohmic electrical contact, between the nickel and the 4H-SiC bulk surface. Following the initial anneal, a second RCA cleaning process was performed to remove contaminants that may have been introduced during the annealing process. Then a 100 nm thick, circular, 3 mm diameter nickel Schottky contact was then deposited on the epitaxial surface. A 10-nm corrosion resistant platinum layer was then deposited on the nickel to serve as a corrosion barrier and to prevent alloying of uranium with the nickel Schottky contact. The die was then annealed at 650°C to form an adequate Schottky barrier contact, between the nickel and the epitaxial 4H-SiC surface. Figure 10 shows the detector structure and the two-steps approach for measurement of actinides within the salt of an electrorefiner.

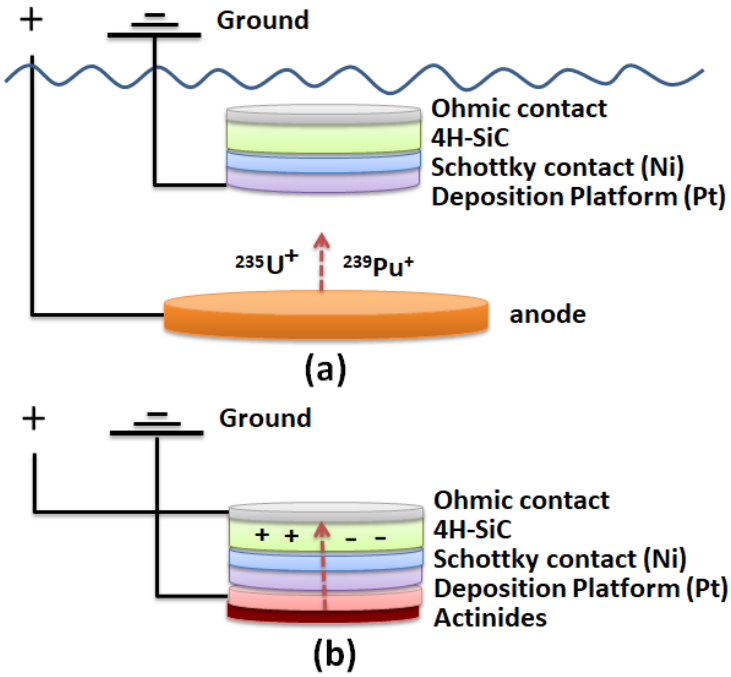

Figure 10. The proposed sensor structure for actinide measurement, (a) electrodepositing step in the salt, (b) measurement step outside the salt, where alpha particles from actinides are collected.

Alpha Spectroscopy at Room Temperature

Measurements of the alpha spectrum of an ^{241}Am disc source using fabricated SiC sensors were performed in bell-jar vacuum at a pressure of <3 mTorr. The negative bias voltage was supplied by a probe that was placed in physical contact with the Schottky contact of the detector and was

connected to the center conductor of a BNC cable in a vacuum. A ground connection was established by placing the detector on the surface of an Inconel substrate heater, such that the ohmic contact of the detector was in contact with the heater surface. A micro-positioner probe was placed in contact with the heater surface and was connected to the outer conductor of the BNC cable, which was connected with a vacuum feedthrough to an Ortec 142B preamplifier.

The detectors were irradiated in a bell jar, using a 1.88 µCi Eberline ^{241}Am alpha source. The source was mounted 5 cm away from the detector, using an aluminum collimator placed in front of the source to form a beam that was perpendicularly incident upon the detector surface. To perform heated measurements, the detector was mounted on a Blue Wave Inconel Substrate heater inside the bell jar. The detector response at room temperature was measured first vs increasing bias voltage from 0 to -200 volts. At each voltage, the alpha spectrum from the ^{241}Am source was measured over a 15-minute counting time. In this case, as the applied voltage increases, the centroid position of the measured spectra shifts to higher channels, as shown in Figure 11. This right-shift in channel number is due to the increased depletion region when bias is raised. The increase in freed charge in the depleted region leads to an increase in the charge induced at the contacts and, thus, a shift in the channel number. Also, the energy resolution improves as the applied voltage increases, because the statistical improvement due to the enlarged number of charge carriers that are collected.

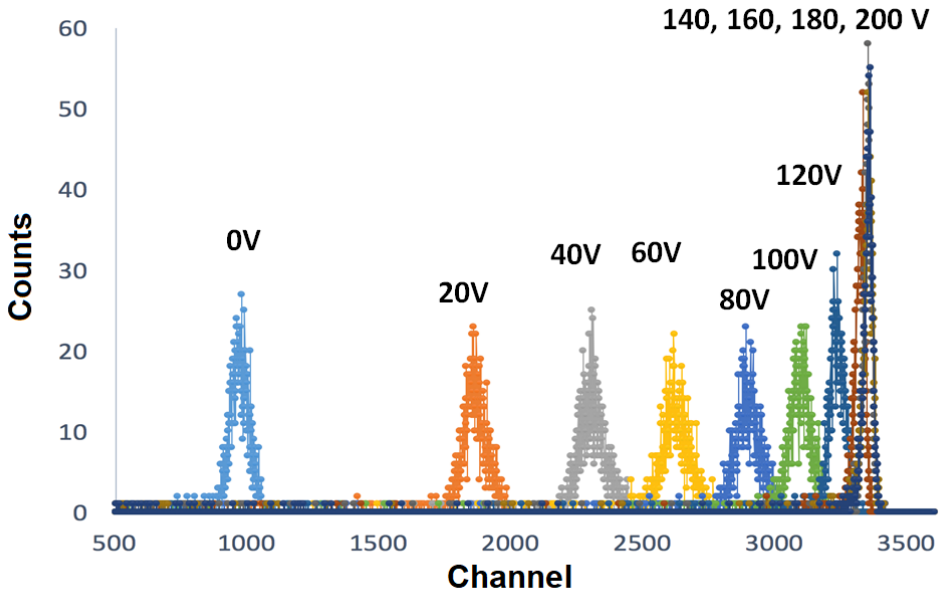

Figure 11. Alpha spectra measured with a 4H-SiC alpha detector at room tmeperatre with increasing bias. As applied voltage is increased, energy resolution improves and the centroid shifts to higher channels.[29]

Experimental Results and Discussion at High Temperture and after Salt Immersion

The detectors were then heated in the vacuum bell jar when being irradiated with an ^{241}Am source. The ^{241}Am spectrum was measured with the detector operated at -200 volts. Spectra were collected at room temperature and then from 100°C to 500°C in 100°C increments (only three temperature

responses of SiC sensor are shown in Figure 12 for clarity). The shift in the centroid position to higher channel numbers with increasing temperature can be explained by the decrease of the SiC W-value, the energy required to create one electron-hole pair in the material, due to the elevated temperature. The centroid and energy resolution of the alpha spectra collected by the heated detector at each temperature were calculated. The energy resolution degraded slightly with increasing temperature and the energy resolution at 500° C was found to be 2.25% at 5.486 MeV. This is an improvement over previous designs using a Ni-Ti-Au design.[27] The previous devices most likely failed due to degradation of the Schottky contact due to diffusion of the metal layers. While the device is stable under a constant operation parameter, its longevity against the thermal expansion/contraction cycles has not been evaluated.

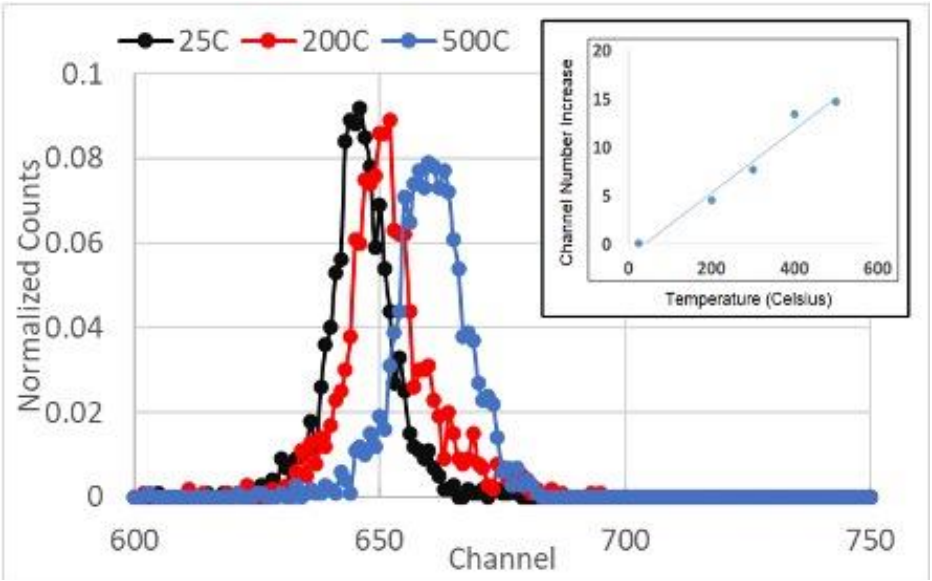

Figure 12. Spectra collected at increased temperatures from room temperature to 500 °C exhibiting an increased centroid location due to a larger amount of charge being freed per energy lost by incident ionizing particles. Inset: Centroid channel number of the measured alpha spectra increases with increasing temperature.

A similar style SiC sensor was packaged (see Figure 13.a for its structure) and immersed in a molten salt within crucible of a benchtop furnace (see Figure 13.b for experimental setup). The detector had uranium electrodeposited onto the surface of the packaged detector. After plating, the detector was pulled out of salt and measured for alpha spectrum as a result of uranium deposited onto its surface. It successfully produced an alpha spectrum (See figure 13.c) with a sufficient resolution that the data could be used to determine the isotopic concentration of the deposited uranium, which was representative of the uranium within the salt.[30] Using the integrated count and the specific activity per unit mass of ^{234}U and ^{238}U, the isotopic concentration of each isotope and the activity ratio of ^{234}U to ^{238}U of the sample was determined as $\cong 0.089 \pm 0.007$. This ratio allows

one to determine that this source comes from a depleted uranium, since in natural uranium the activity ratio should be 0.99.

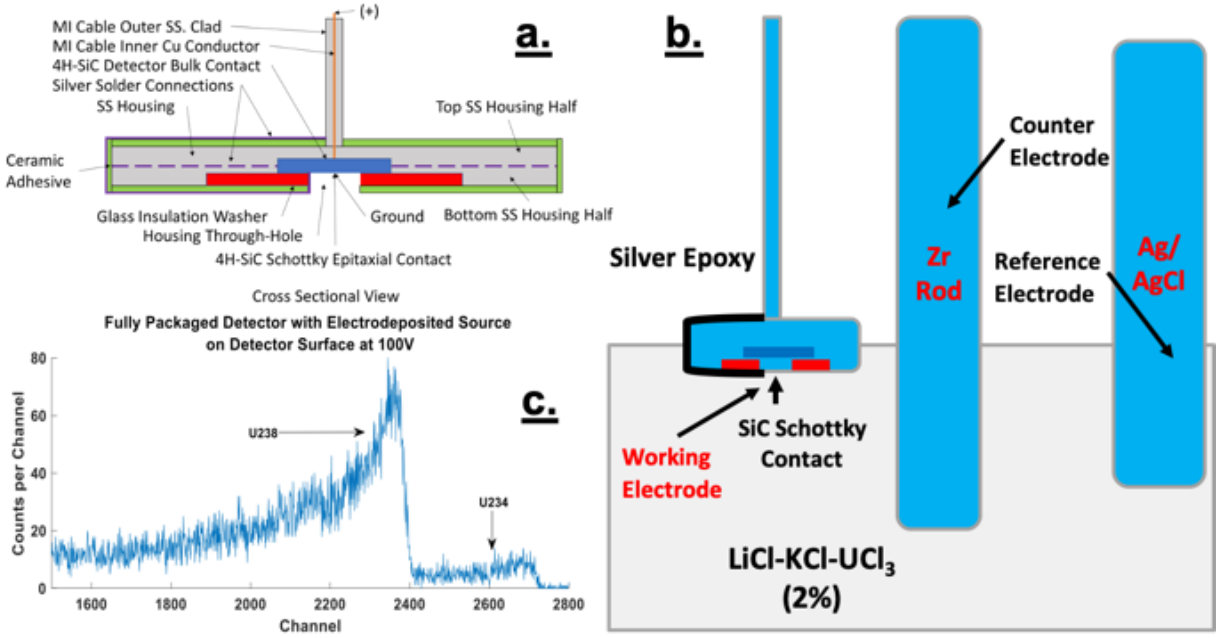

Figure 13. Demonstration of actinide quantification and isotope determination by SiC in molten salt for pyroprocessing. (a) the structure of an in-house fabricated SiC sensor in its electrical and thermal insulation package; (b) a packaged SiC sensor is merged into molten salt for electrodeposition of uranium onto SiC; (c) the measured alpha spectrum used to determine the $^{234}U/^{238}U$ ratio, which is 0.089±0.007.

Conclusions

Several techniques for the integration of NDA measurements into the overall safeguards approach for pyroprocessing facilities were examined. Some of the applicable approaches were integrated in the safeguards modeling aspect of the Virtual Facility Distributed Test Bed. Pyroprocessing plants have unique features and measurements which may play into an overall plant monitoring approach, but more work is needed to quantify how these approaches will improve an overall safeguards approach.

Preliminary results on the efficacy of NDA techniques using conventional detectors via difference in gamma counts per second show, as the lower limits of detection, a 99% confidence in detecting a 0.2 SQ protracted electrorefiner diversion over the course of one year, and a 99% confidence in detecting a 1.4 SQ protracted transuranic diversion of the course of one year. This work will be expanded upon in future efforts.

4H-SiC diodes were fabricated and tested, with the goal of developing a packaged detector that would function in a high temperature environment, following submersion in high temperature molten salts, with sufficient resolution for actinide detection, identification, and tracking in a molten salt electrorefiner. The detectors were tested at elevated temperatures to simulate the molten salt environment. The energy resolution of the Ni-Pt Schottky contact design that is

described herein was able to achieve resolution at 500° C as 2.25% at 5.486 MeV. A shift in centroid position of alpha spectra to higher channel numbers was measured at increasing temperatures. The sensor has been successfully packaged into a rugged format and tested in an emerged salt environment for uranium isotope detection.

Keywords
Electrochemical; Pyroprocessing; Safeguards; NDA; Process Monitoring; Data Analytics

Acknowledgements
This research was performed using funding received from the U.S Department of Energy, Office of Nuclear Energy's Nuclear Energy University Program. Sandia National Laboratories is a multimission laboratory managed and operated by National Technology and Engineering Solutions of Sandia, LLC, a wholly owned subsidiary of Honeywell International Inc., for the U.S. Department of Energy's National Nuclear Security Administration under contract DE-NA0003525, SAND2020-8720J.

Author Biographies
Noah Harris is an MS candidate in Radiation Health Physics at Oregon State University and has obtained a BS in Physics from Western Washington University. His interests include nuclear science, machine learning, and quantum information.

Haori Yang is an Associate Professor at Oregon State University. He holds a PhD in Nuclear Engineering and Radiological Sciences from the University of Michigan and MS/BS in Engineering Physics from Tsinghua University.

Jianbang Ge holds his PhD and BS in Metallurgy Engineering from University Science and Technology Beijing. His research activities include work on molten salt anode/silicon film preparation and electrochemical separation of fission products/rotating disk electrode in molten salt.

Jinsuo Zhang is a professor in the Nuclear Engineering Program at Virginia Tech. He holds a Ph.D and B.S. from Zhejiang University and B.S. from Zhejiang University. Prof. Zhang is the director of the Nuclear Materials and Fuel Cycle Research Center. His research focuses on studies of advanced used nuclear fuel reprocessing, safeguards and non-proliferation, nuclear materials, material compatibility and materials corrosion in advanced and current nuclear reactors

Jamie Coble is an Associate Professor, Southern Company Faculty Fellow, and Assistant Department Head of Undergraduate Studies and Service in Nuclear Engineering at the University of Tennessee, Knoxville. Her research focuses on data analytics and statistical analysis for process and equipment monitoring, anomaly detection, and prognostics.

Steve Skutnik is an R&D staff member in the Reactor and Nuclear Systems Division at Oak Ridge National Laboratory. He was previously a professor at the University of Tennessee Knoxville.

Neil Taylor obtained a BS in Engineering Physics with a specialization in Nuclear Engineering, a MS in Nuclear Engineering and is currently pursuing a PhD student at The Ohio State University. His work focuses on using 3D printing to fabricate nuclear insutrmentation and sensors.

Joshua Jarrell is a post-doctoral researcher at Lawrence Livermore National Laboratory. He received a PhD in Nuclear Engineering from The Ohio State University and his current research focuses on radioisotope batteries and radiation hardness of materials.

Thomas Blue is an Emeritus Academy Professor of Nuclear Engineering at The Ohio State University with a PhD degree in Nuclear Engineering from the University of Michigan. His research focus is the development of instrumentation for advanced reactors and its testing at high temperatures in radiation fields.

Lei R. Cao is a Professor in Nuclear Engineering Program at The Ohio State University with a PhD degree from the Nuclear and Radiological Engineering Program at University of Texas at Austin. His major research focuses on sensor and instrumentation for nuclear energy and non-proliferation applications.

Michael Simpson is a Professor of Materials Science & Engineering at the University of Utah. He holds a PhD in chemical engineering from Princeton University and a BS in chemical engineering from California Institute of Technology. His research focuses on molten salt chemistry and dry processing methods for reprocessing nuclear fuel.

Ben Cipiti is a Principle Member of the Technical Staff at Sandia National Laboratories. He holds a PhD in Nuclear Engineering from the University of Wisconsin-Madison and BS in Mechanical Engineering from Ohio University.

Nathan Shoman obtained a BS and MS in Nuclear Engineering from the University of Tennessee. He currently works as a Member of the Technical Staff at Sandia National Laboratories where his research focuses on applied machine learning for safeguards and security applications.

References

1. Croce, M. et al. 2021. Electrochemical Safeguards Measurement Technology Development at LANL, *J. Nucl. Mater. Manage*, Vol. X, No. X.
2. Garcia, H. et al. 2002. Proliferation resistance of advanced sustainable nuclear fuel cycles, *Nuclear Plant Journal*, Vol 20, No. 1.
3. Orton, C.R. et al. 2011. Proof of Concept Simulations of the Multi-Isotope Process Monitor: An Online, Nondestructive, Near-Real-Time Safeguards Monitor for Nuclear Fuel Reprocessing Facilities, *Nuclear Instruments and Methods in Physics Research Section A: Accelerators, Spectrometers, Detectors and Associated Equipment*, Vol. 629, No. 1.

4. Wise, B.M. and Gallagher, N.B. 1996. The Process Chemometrics Approach to Process Monitoring and Fault Detection, *Journal of Process Control*, Vol. 6, No. 6.
5. Cipiti, B.B. et al. 2012. Modeling and Design of Integrated Safeguards and Security for an Electrochemical Reprocessing Facility. SAND2012-9303, Sandia National Laboratories.
6. Coble, J.B. et al. 2020. Review of Candidate Techniques for Material Accountancy Measurements in Electrochemical Separations Facilities, *Nuclear Technology*, Vol. 2020.
7. Skutnik, S.E. et al. 2018. A Signatures-Based Approach to Electrochemcial Reprocessing Safeguards Modeling & Evaluation, in *Advances in Nonproliferation Technology and Policy Conference (ANTPC)*, Orlando, FL.
8. Gilliam, S.N. 2018. Candidate Measurement Technique Application as a Method for Materials Accountancy in Electrochemical Reprocessing, Masters Thesis, University of Tennessee-Knoxville.
9. Cooper, M. 2019. Semi-Empirical Modeling and Implementation of Hybrid K-Edge Densitometry for Pyroprocessing Applications, *Nuclear Engineering*, University of Tennessee-Knoxville.
10. Rappleye, D. et al. 2017. Electroanalytical measurements of binary-analyte mixtures in molten LiCl-KCl eutectic: Uranium (III)-and Magnesium (II)-Chloride, *Journal of Nuclear Materials*, Vol. 486, 369-380.
11. Pouri, S. R. 2017. Comparative Studies of Diffusion Models and Artificial Neural Intelligence on Electrochemical Process of U and Zr Dissolutions in LiCl-KCl Eutectic Salts, PhD Thesis, Virginia Commonwealth University.
12. Mitchell, J. 2020. Determining the Feasibility of Cyclic Voltammetry for Pyroprocessing Safeguards, Master's Thesis, University of Tennessee.
13. Haori, Y., Zhang, J., & Cipiti, B. 2018. Integration of Nuclear Material Accounting Data and Process Monitoring Data for Improvement on Detection Probability in Safeguarding Electrochemical Processing Facilities. Nuclear Energy University Programs. doi: 18-15043.
14. Horne, S. et al. 2016. GADRAS-DRF 18.6 User's Manual, SAND2016-4345, Sandia National Laboratories.
15. Knoll, G.F. 2010. Radiation detection and measurement. New Jersey: John Wiley & Sons.
16. Phillips, J. et al. 1978. Glassy Carbon Rotating Ring-Disc Electrode for Molten Salt Studies, *Analytical Chemistry*, Vol. 48, 1266-1248.
17. Tran, Q.T., et al. 2014. Optimization of Actinides Trace Precipitation on Diamond/Si PIN Sensor for Alpha-Spectrometry in Aqueous Solution, *IEEE Transitions in Nuclear Science*, Vol. 99.
18. Wang, Z. H., Rappleye, D., & Simpson, M. F. 2016. Voltammetric Analysis of Mixtures of Molten Eutectic LiCl-KCl Containing LaCl3 and ThCl4 for Concentration and Diffusion Coefficient Measurement, *Electrochimica Acta*, Vol. 191.
19. Li, S. X., Johnson, T. A., Westphal, B. R., Goff, K. M., & Benedict, R. W. 2005. Electrorefining Experience for Pyrochemical Reprocessing of Spent EBR-II Driver Fuel, INL/CON-05-00305, Idaho National Laboratory.
20. Kemmer, J. 1980. Fabrication of Low Noise Silicon Radiation Detectors by the Planar Process, *Nuclear Instruments and Methods*, Vol. 169, No. 3.
21. Cheung, R. 2006. Silicon Carbide Microelectromechanical Systems for Harsh Environments, World Scientific.

22. Ruddy, F. H., Dulloo, A. R., Seidel, J. G., Seshadri, S., & Rowland, L. B. 1998. Development of a Silicon Carbide Radiation Detector, *IEEE Transactions on Nuclear Science*, Vol. 45, No. 3.
23. Bertuccio, G., Casiraghi, R., & Nava, F. 2001. Epitaxial Silicon Carbide for X-ray Detection, *IEEE Transactions on Nuclear Science*, Vol. 28, No. 2.
24. Bertuccio, G. 2005. Prospect for Energy Resolving X-ray Imaging with Compound Semiconductor Pixel Detectors, *Nuclear Instruments and Methods in Physics Research Section A: Accelerators, Spectrometers, Detectors and Associated Equipment*, Vol. 546.
25. Tung, R. T. 2014. The Physics and Chemistry of the Schottky Barrier Height, *Applied Physics Reviews*, Vol. 1, No. 1.
26. Zat'ko, B., Dubecký, F., Šagátová, A., Sedlačová, K., & Ryć, L. 2015. High Resolution Alpha Particle Detectors Based on 4H-SiC Epitaxial Layer, *Journal of Instrumentation*, Vol. 10, No. 4.
27. Garcia, T. R., Kumar, A., Reinke, B., Blue, T. E., & Windl, W. 2013. Electron-Hole Pair Generation in SiC High-Temperature Alpha Particle Detectors. *Applied Physics Letters*, Vol. 103, No. 15.
28. Kern, W. 1990. The Evolution of Silicon Wafer Cleaning Technology, *Journal of the Electrochemical Society*, Vol. 137, No. 6.
29. Wang, L., Jarrell, J., Xue, S., Tan, C., Blue, T., & Cao, L. R. 2018. Fast Neutron Detection at Near-Core Location of a Research Reactor with a SiC Detector, *Nuclear Instruments and Methods in Physics Research Section A: Accelerators, Spectrometers, Detectors and Associated Equipment*, Vol. 888.
30. Taylor, N. R., Alnajjar, N., Jarrell, J., Kandlakunta, P., Simpson, M., Blue, T. E., & Cao, L. R. 2019. Isotopic Concentration of Uranium from Alpha Spectrum of Electrodeposited Source on 4H-SiC Detector at 500° C, *Journal of Radioanalytical and Nuclear Chemistry*, Vol. 320, No. 2.